

# Synthesis and characterization of some Mn(II) and Mn(III) complexes of *N,N'*-*o*-phenylenebis(salicylideneimine)(LH<sub>2</sub>) and *N,N'*-*o*-phenylenebis(5-bromosalicylideneimine)(L'H<sub>2</sub>). Crystal structures of [Mn(L)(H<sub>2</sub>O)(ClO<sub>4</sub>)], [Mn(L)(NCS)] and an infinite linear chain of [Mn(L)(OAc)]

Subhendu Biswas<sup>a</sup>, Kamala Mitra<sup>a</sup>, C.H. Schwalbe<sup>c</sup>, C. Robert Lucas<sup>b,\*</sup>,  
Shyamal K. Chattopadhyay<sup>a,\*</sup>, Bibhutosha Adhikary<sup>a,\*</sup>

<sup>a</sup> Department of Chemistry, Bengal Engineering and Science University, Shibpur, Howrah 711 103, India

<sup>b</sup> Department of Chemistry, Memorial University of Newfoundland, St. John's, Newfoundland, Canada A1B 3X7

<sup>c</sup> Department of Pharmaceutical Sciences, Aston University, Aston Triangle, Birmingham B4 7ET, UK

Received 20 July 2004; accepted 14 January 2005

Available online 14 March 2005

## Abstract

A series of manganese(II) [Mn(L)] and manganese(III) [Mn(L)(X)] (X = ClO<sub>4</sub>, OAc, NCS, N<sub>3</sub>, Cl, Br and I) complexes have been synthesized from Schiff base ligands *N,N'*-*o*-phenylenebis(salicylideneimine)(LH<sub>2</sub>) and *N,N'*-*o*-phenylenebis(5-bromosalicylideneimine)(L'H<sub>2</sub>) obtained by condensation of salicylaldehyde or 5-Br salicylaldehyde with *o*-phenylene-diamine. The complexes have been characterized by the combination of IR, UV–Vis spectroscopy, magnetic measurements and electrochemical studies. Three manganese(III) complexes **3** [Mn(L)(ClO<sub>4</sub>)(H<sub>2</sub>O)], **5** [Mn(L)(OAc)] and **13** [Mn(L)(NCS)] have been characterized by X-ray crystallography. The X-ray structures show that the manganese(III) is hexa-coordinated in **3**, it is penta-coordinated in **13**, while in **5** there is an infinite chain where the MnL moieties are connected by acetate ions acting as bridging bidentate ligand. The cyclic voltammograms of all the manganese(III) complexes exhibit two reversible/quasi-reversible/irreversible responses assignable to Mn(III)/Mn(II) and Mn(IV)/Mn(III) couples. It was observed that the ligand L'H<sub>2</sub> containing the 5-bromosal moiety always stabilizes the lower oxidation states compared to the corresponding unsubstituted LH<sub>2</sub>. Cyclic voltammograms of the manganese(II) complexes (**1** and **2**) exhibit a quasi-reversible Mn(III)/Mn(II) couple at *E*<sub>1/2</sub> –0.08 V for **1** and 0.054 V for **2**.

© 2005 Elsevier B.V. All rights reserved.

**Keywords:** Manganese(II) and manganese(III) complexes; Phenolate Schiff bases; N<sub>2</sub>O<sub>2</sub> donors; Acetate bridged manganese(III) chain; Electronic spectra; X-ray structure; Electrochemistry

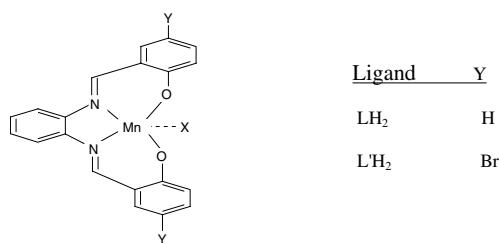
## 1. Introduction

There has been considerable interest in the coordination chemistry of manganese involving nitrogen and oxygen donor ligands due to the increasing recognition

of the role of this metal in biological systems [1–4]. Studies of spectroscopic and physicochemical properties along with X-ray structure determination of model complexes are especially important to gain insights into the nature and mode of action of the manganese containing prosthetic groups. It has been established that the biological sites containing manganese are of variable nuclearity and the oxidation states of manganese vary between +2 and +5 [5–11]. Of particular interest is the

\* Corresponding authors. Fax: + 91 33 2668 2916.

E-mail addresses: [shyamal@chem.becs.ac.in](mailto:shyamal@chem.becs.ac.in) (S.K. Chattopadhyay), [adhikarybibhu@yahoo.com](mailto:adhikarybibhu@yahoo.com) (B. Adhikary).



Scheme 1.

study of electron transfer behavior of manganese(II), manganese(III) and manganese(IV) and its modulations by change of substituents on ligand because of their potential uses as oxidizing agents, catalysts [11–13] and electro catalysts [14–16] for the oxidation of compounds such as alcohols, esters and water [17–19]. In this paper, we report synthesis, electronic spectra and redox activities of several manganese(II) and manganese(III) complexes and structural characterization of three manganese(III) complexes involving N<sub>2</sub>O<sub>2</sub> Schiff-base ligand (see Scheme 1).

## 2. Experimental

### 2.1. Materials

All the chemicals and solvents used for the syntheses were of commercially available reagent grade and were used without further purification. TEAP was prepared following the literature procedure [20]. All the Schiff base ligands were prepared by known methods [21].

### 2.2. Synthesis of the complexes

#### 2.2.1. Complexes (3, 4, 5, 6, 7 and 8)

All of these were prepared by a similar method given below.

The complexes were prepared by stirring a MeCN solution (25 ml) of ligand (1 mmol, LH<sub>2</sub>/L'H<sub>2</sub>) and adding successively a MeCN solution (5 ml) of Mn(ClO<sub>4</sub>)<sub>2</sub> · 6H<sub>2</sub>O/Mn(OAc)<sub>2</sub> · 4H<sub>2</sub>O/MnCl<sub>2</sub> · 6H<sub>2</sub>O (1 mmol) and Et<sub>3</sub>N (2 mmol) in 5 ml MeCN in stirring condition. The initial yellow color of the solution rapidly changed to brown. After 3 h of stirring at room temperature slow evaporation of solvent lead to deposition brown compounds. The products were collected by filtration and washed with ethanol–diethyl ether mixture (1:1). The compounds were recrystallized from MeCN–diethyl ether mixture. Yield ranges from 80% to 91%.

#### 2.2.2. Complexes (9, 10, 11, 12, 13, 14 and 15)

The complexes were prepared by stirring a MeCN solution (25 ml) of ligand (1 mmol, LH<sub>2</sub>/L'H<sub>2</sub>) and adding successively a MeCN solution (5 ml) of

Mn(ClO<sub>4</sub>)<sub>2</sub> · 6H<sub>2</sub>O/Mn(OAc)<sub>2</sub> · 4H<sub>2</sub>O/MnCl<sub>2</sub> · 6H<sub>2</sub>O (1 mmol) and Et<sub>3</sub>N (2 mmol) in 5 ml MeCN in stirring condition. After 1 h of stirring, a saturated aqueous solution (5 ml) of KBr/KI/NH<sub>4</sub>NCS/NaN<sub>3</sub> was added which results in immediate separation of brown/black colored corresponding compounds. They were collected by filtration and washed with water, ethanol and finally with diethyl ether. All the compounds were recrystallized from MeCN–ether mixture, except 9 and 10, which cannot be purified further due to its solubility only in DMF and DMSO. Yield ranges from 80% to 94%.

#### 2.2.3. Complexes (1 and 2)

The complexes were prepared by adding solid Mn(ClO<sub>4</sub>)<sub>2</sub> · 6H<sub>2</sub>O (1 mmol) to a degassed MeCN solution (25 ml) of ligand (1 mmol, LH<sub>2</sub>/L'H<sub>2</sub>) and Et<sub>3</sub>N (2 mmol) in 5 ml MeCN at room temperature. Yellow compounds were separated within 20 min. The compounds were collected by filtration under N<sub>2</sub> and washed in acetonitrile and finally with diethyl ether. Yield ranges from 70% to 80%.

*Caution!* Perchlorate salts are potentially explosive, and though we have not encountered any problem, nevertheless they should be handled with care.

### 2.3. Physical measurements

Microanalyses (CHN) were performed on a Perkin–Elmer 2400II elemental analyzer. Electronic spectra were obtained using a JASCO 7850 spectrophotometer. IR spectra were recorded on JASCO FT/IR-460 spectrometer with samples prepared as KBr pellets. Electrochemical experiments were carried out using a EG&G PARC VersaStat II potentiostat with three-electrode configuration consisting of a PARC glassy carbon working electrode, a Pt wire as auxiliary electrode and Ag/AgCl as the reference electrode and 0.1 mol dm<sup>-3</sup> NEt<sub>4</sub>ClO<sub>4</sub> as supporting electrolyte in MeCN or DMF solution under dry nitrogen atmosphere with a scan rate 0.1 V s<sup>-1</sup>. Data were collected using 'ECHEM' software supplied by PARC. For electrochemical and spectral measurements HPLC grade solvents were used. All the electrochemical potentials were calibrated against a ferrocene–ferrocenium couple. Room temperature magnetic susceptibility measurements were done by PAR 155 model vibrating sample magnetometer, which was calibrated against Hg[Co(NCS)<sub>4</sub>].

#### 2.4. Crystal structure determination and structural refinement of 3, 5 and 13

The single crystals of 3, 5 and 13 suitable for X-ray diffraction were grown by slow diffusion of anhydrous diethyl ether into a MeCN solution of the appropriate compound at room temperature. Crystal data are summarized in Table 3. Intensity data were collected on a

Nonius  $\kappa$ -geometry based CAD4/PC V2.0 X-ray diffractometer for **3** and in a Bruker P<sub>4</sub>/CCD system for **5** and **13**, using graphite monochromated Mo K $\alpha$  radiation in all cases. For **3**, absorption corrections were derived from psi-scan measurements [22] and Siemens area detected absorption routine SADABS for **5** and **13**. The structures were solved by direct methods [23] refined by least squares using the program SHELXL-97 [24]. The non-hydrogen atoms were refined independently with anisotropic displacement parameters. Most of the hydrogen atoms appeared in difference Fourier maps. For **3**, water hydrogen atoms were refined independently, subject to a distance restraint. All other hydrogen atoms for **3** and all hydrogens for **5** and **13** were placed at calculated positions and refined using a riding model with isotropic displacement parameters. The refinements converged with the residuals summarized in Table 3. Selected bond distances are given in Table 4.

### 3. Results and discussion

#### 3.1. Synthesis

The manganese(II) complexes **1** and **2** have been prepared in fairly good yields (70–80%) by reacting solid  $\text{Mn}(\text{ClO}_4)_2 \cdot 6\text{H}_2\text{O}$  with the appropriate ligand in nitrogen atmosphere. The solutions of these two complexes are not stable in air and turn deep chocolate immediately due to aerial oxidation. All the manganese(III) complexes have been prepared by the direct reaction of corresponding ligands and the manganese(II) salts in presence of  $\text{Et}_3\text{N}$  in aerobic condition, when the initially formed manganese(II) complexes rapidly oxidizes to the corresponding manganese(III) species, probably following similar mechanism as described by Boucher and Coe [25].

We have also synthesized the same manganese(III) complexes using the saturated ligand obtained by the reduction of the Schiff-base ligand ( $\text{LH}_2$ ) by  $\text{NaBH}_4$ . The complexes obtained from the saturated ligand are oxidized to original Schiff-base ligand during preparation of the complexes, which was confirmed by infrared spectroscopy (absence of N–H band at ca.  $3200\text{ cm}^{-1}$ ) as well as by X-ray structure determination of one of the representative compound (the acetate coordinated derivative). Earlier workers also reported similar observations [26] (see Table 2).

#### 3.2. Description of the structures

##### 3.2.1. Complex **3** [ $\text{MnL}(\text{ClO}_4)(\text{H}_2\text{O})$ ]

The structural analysis of complex **3** (Fig. 1) has revealed that the central manganese(III) ion adopts a distorted octahedral structure. The  $\text{N}_2\text{O}_2$  donor set coming from ligand itself forms an equatorial plane, and the

Table 1  
List of the complexes reported in this paper

	Complex	X	Y
<b>1</b>	$\text{Mn}(\text{L})(\text{H}_2\text{O})$		H
<b>2</b>	$\text{Mn}(\text{L}')(\text{H}_2\text{O})$		Br
<b>3</b>	$[\text{Mn}(\text{L})(\text{ClO}_4)(\text{H}_2\text{O})]$	$\text{ClO}_4$	H
<b>4</b>	$[\text{Mn}(\text{L}')(\text{ClO}_4)(\text{H}_2\text{O})] \cdot 3\text{H}_2\text{O}$	$\text{ClO}_4$	Br
<b>5</b>	$[\text{Mn}(\text{L})(\text{OAc})]$	OAc	H
<b>6</b>	$[\text{Mn}(\text{L}')(\text{OAc})] \cdot 2\text{H}_2\text{O}$	OAc	Br
<b>7</b>	$[\text{Mn}(\text{L})(\text{Cl})(\text{H}_2\text{O})]$	Cl	H
<b>8</b>	$[\text{Mn}(\text{L}')(\text{Cl})(\text{H}_2\text{O})]$	Cl	Br
<b>9</b>	$[\text{Mn}(\text{L})(\text{Br})(\text{H}_2\text{O})]$	Br	H
<b>10</b>	$[\text{Mn}(\text{L}')(\text{Br})(\text{H}_2\text{O})]$	Br	Br
<b>11</b>	$[\text{Mn}(\text{L})(\text{I})(\text{H}_2\text{O})]$	I	H
<b>12</b>	$[\text{Mn}(\text{L}')(\text{I})(\text{H}_2\text{O})]$	I	Br
<b>13</b>	$[\text{Mn}(\text{L})(\text{NCS})]$	NCS	H
<b>14</b>	$[\text{Mn}(\text{L})(\text{N}_3)]$	$\text{N}_3$	H
<b>15</b>	$[\text{Mn}(\text{L}')(\text{N}_3)]$	$\text{N}_3$	Br

Table 2  
Analytical data and magnetic moments for the complexes

Complex	Analyses: Calc. (found)			$\mu_{\text{eff}}$ (BM)
	C (%)	H (%)	N (%)	
<b>1</b>	62.00(62.10)	4.13(4.11)	7.24(7.23)	5.92
<b>2</b>	44.03(44.02)	2.57(2.56)	5.14(5.13)	6.01
<b>3</b>	49.33(49.32)	3.29(3.28)	5.76(5.77)	4.62
<b>4</b>	34.36(34.35)	2.86(2.87)	4.01(4.02)	4.75
<b>5</b>	61.68(61.67)	3.97(3.86)	6.54(6.55)	3.84
<b>6</b>	42.44(42.45)	3.05(3.04)	4.50(4.51)	3.82
<b>7</b>	56.80(56.81)	3.79(3.78)	6.63(6.62)	4.97
<b>8</b>	41.34(41.35)	2.41(2.42)	4.82(4.81)	4.88
<b>9</b>	51.39(51.40)	3.43(3.42)	5.99(5.98)	4.94
<b>10</b>	38.40(38.41)	2.24(2.25)	4.48(4.47)	4.87
<b>11</b>	46.69(46.70)	3.11(3.10)	5.45(5.46)	4.69
<b>12</b>	35.71(35.72)	2.08(2.07)	4.17(4.16)	4.77
<b>13</b>	59.01(59.00)	3.27(3.26)	9.83(9.84)	4.98
<b>14</b>	58.39(58.40)	3.41(3.40)	17.03(17.02)	4.88
<b>15</b>	42.18(42.17)	2.11(2.10)	12.30(12.22)	4.74

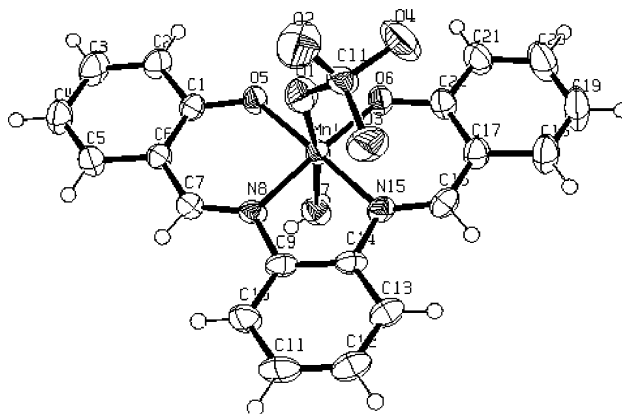


Fig. 1. ORTEP diagram for the complex **3** [ $\text{Mn}(\text{L})(\text{ClO}_4)(\text{H}_2\text{O})$ ] showing the atom labeling scheme and 50% probability ellipsoid for the non-hydrogen atom.

Table 3  
Data collection and structure refinements for **3**, **5** and **13**

Complex	<b>3</b>	<b>5</b>	<b>13</b>
Empirical formula	MnC <sub>20</sub> H <sub>16</sub> N <sub>2</sub> O <sub>7</sub> Cl	C <sub>22</sub> H <sub>17</sub> N <sub>2</sub> O <sub>4</sub> Mn	C <sub>21</sub> H <sub>14</sub> N <sub>3</sub> O <sub>2</sub> MnS
Formula weight	486.74	428.33	427.36
Crystal color, habit	red, plate	black, prism	black, plate
Crystal dimensions (mm)	0.35 × 0.25 × 0.08	0.78 × 0.30 × 0.14	0.50 × 0.24 × 0.04
Crystal system	triclinic	monoclinic	monoclinic
<i>a</i> (Å)	8.0481(11)	11.4055(6)	12.8465(4)
<i>b</i> (Å)	11.2063(19)	14.1242(7)	10.0590(3)
<i>c</i> (Å)	11.844(2)	12.4671(6)	14.1869(4)
$\alpha$ (°)	98.555(13)	90	90
$\beta$ (°)	109.329(14)	115.2240(9)	100.0050(5)
$\gamma$ (°)	93.359(13)	90	90
<i>V</i> (Å <sup>3</sup> )	990.1(3)	1816.9(1)	1805.39(8)
Space group	<i>P</i> $\bar{1}$	<i>P</i> 2 <sub>1</sub> / <i>n</i> (#14)	<i>P</i> 2 <sub>1</sub> / <i>n</i> (#14)
<i>Z</i> value	2	4	4
$\mu$ (Mo K $\alpha$ ) (mm <sup>-1</sup> )	0.849	0.760	0.870
<i>T</i> <sub>max,min</sub>	0.934, 0.737	0.5886, -0.194	0.6702, 0.9660
<i>F</i> (0 0 0)	496	880	872
Index ranges	-9 ≤ <i>h</i> ≤ 1, -13 ≤ <i>k</i> ≤ 13, -14 ≤ <i>l</i> ≤ 14	-14 ≤ <i>h</i> ≤ 14, -17 ≤ <i>k</i> ≤ 17, -15 ≤ <i>l</i> ≤ 15	-16 ≤ <i>h</i> ≤ 16, -12 ≤ <i>k</i> ≤ 12, -17 ≤ <i>l</i> ≤ 17
Data/restraints/parameters	3443/2/289	3714/0/262	3687/0/253
<i>R</i> <sub>1</sub> ; <i>R</i> <sub>w</sub>	0.0384; 0.1104	0.029; 0.082	0.029; 0.078
Maximum and minimum peak in difference map (e Å <sup>-3</sup> )	0.66 and -0.39	0.337 and -0.194	0.354 and -0.170
Goodness-of-fit on <i>F</i> <sup>2</sup>	1.012	1.049	1.053

remaining axial positions are occupied by the O donor set of H<sub>2</sub>O and perchlorate. The bond distances of Mn(1)–O(1) and Mn(1)–O(7) (2.3684 and 2.2370 Å, respectively) are longer than those of Mn(1)–O(5), Mn(1)–O(6), Mn(1)–N(8) and Mn(1)–N(15) (1.8770,

1.8458, 1.9729, 1.9755 Å, respectively) which fall within the range observed for structurally characterized manganese(III) compounds [27].

The elongated axial bonds may have arisen from the Jahn–Teller effect. The basal bond angles are all close to

Table 4  
Selected bond distances (Å) and bond angles (°) for complexes **3**, **5** and **13**

<b>3</b>		<b>5</b>		<b>13</b>	
<i>Bond distances</i>					
Mn(1)–O(5)	1.877(2)	Mn(1)–O(1)	1.8777(12)	Mn(1)–O(1)	1.8562(11)
Mn(1)–O(6)	1.846(2)	Mn(1)–O(2)	1.8762(12)	Mn(1)–O(2)	1.8886(11)
Mn(1)–O(1)	2.368(3)	Mn(1)–O(3)	2.2166(12)	Mn(1)–N(1)	1.9949(13)
Mn(1)–O(7)	2.238(3)	Mn(1)–O(4a)	2.2432(12)	Mn(1)–N(2)	1.9840(13)
Mn(1)–N(8)	1.973(3)	Mn(1)–N(1)	1.9969(15)	Mn(1)–N(3)	2.1649(15)
Mn(1)–N(15)	1.976(3)	Mn(1)–N(2)	1.9972(15)		
<i>Bond angles</i>					
N(8)–Mn(1)–N(15)	82.83(11)	N(1)–Mn(1)–N(2)	82.05(6)	N(1)–Mn(1)–N(2)	82.29(5)
N(8)–Mn(1)–O(1)	83.25(10)	N(1)–Mn(1)–O(1)	93.24(5)	N(1)–Mn(1)–O(1)	91.58(5)
N(8)–Mn(1)–O(7)	86.12(10)	N(1)–Mn(1)–O(2)	173.95(5)	N(1)–Mn(1)–O(2)	170.47(5)
N(15)–Mn(1)–O(1)	89.31(10)	N(1)–Mn(1)–O(3)	83.45(5)	N(1)–Mn(1)–N(3)	89.37(5)
N(15)–Mn(1)–O(7)	91.24 (10)	N(1)–Mn(1)–O(4)	89.62(5)	N(2)–Mn(1)–N(3)	96.41(6)
O(5)–Mn(1)–O(6)	90.67(10)	O(1)–Mn(1)–O(2)	92.12(5)	O(1)–Mn(1)–O(2)	90.90(5)
O(5)–Mn(1)–N(8)	93.45(10)	O(1)–Mn(1)–N(2)	173.24(5)	O(1)–Mn(1)–N(3)	99.61(5)
O(5)–Mn(1)–N(15)	174.41(11)	O(1)–Mn(1)–O(3)	96.17(5)	O(1)–Mn(1)–N(2)	162.79(5)
O(5)–Mn(1)–O(1)	86.10(10)	O(1)–Mn(1)–O(4)	94.45(5)	O(2)–Mn(1)–N(2)	92.72(5)
O(5)–Mn(1)–O(7)	92.67(10)	O(2)–Mn(1)–N(2)	92.85(5)	O(2)–Mn(1)–N(3)	99.28(5)
O(6)–Mn(1)–N(8)	175.56(10)	O(2)–Mn(1)–O(3)	93.17(5)		
O(6)–Mn(1)–N(15)	92.94(11)	O(2)–Mn(1)–O(4)	92.78(5)		
O(6)–Mn(1)–O(1)	95.39 (11)	O(3)–Mn(1)–O(4)	167.62(5)		
O(6)–Mn(1)–O(7)	95.35(11)	N(2)–Mn(1)–O(3)	88.13(5)		
O(1)–Mn(1)–O(7)	169.20(10)	N(2)–Mn(1)–O(4)	80.74(5)		

90° (O(5)–Mn–O(6), N(8)–Mn–O(5), N(15)–Mn–O(6) are 90.67°, 93.67°, 92.96°, respectively) except N(15)–Mn–N(8) that is 82.82°. The manganese atom is 0.048(1) Å out of the plane of these four atoms. Compared to the [Mn(L)(ImzH)<sub>2</sub>]ClO<sub>4</sub> complex recently investigated in our laboratories [27], the angles subtended at Mn by equatorial ligand atoms differ by at most 1.2°. The diverse axial ligands in the present case show greater variation and a less ideal geometry, e.g., O(1)–Mn(1)–O(7) is 169.3(1)° while the imidazole N–Mn–N angle was 173.8(1)°. Participation of the perchlorate ion as a ligand is evidently sensitive to conditions. When the identical [Mn<sup>III</sup>(L)]<sup>+</sup> complex, was crystallized from methanol containing a little water, the axial positions were occupied by water and methanol at Mn–O distances of 2.272(2) and 2.292(2) Å [28]. Likewise, the related diaqua-(*N,N'*)-3,5-dichlorobis-(salicylidene)-(1,2-diaminoethane)Mn(III) perchlorate has solvent (water) molecules occupying both axial positions with Mn–O distances 2.220(5) and 2.272(5) Å [29]. With weakly coordinating axial ligands very long Mn–O distances can occur: 2.489(4) Å to one triflate O atom in [(3,3'-17-crown-6-*o*-phsal)Mn(III)](CH<sub>3</sub>COO)Ba(SO<sub>3</sub>CF<sub>3</sub>)<sub>2</sub>·2H<sub>2</sub>O [30]. Although in this series of four N<sub>2</sub>O<sub>4</sub> donor complexes there are differences in detail among the tetradentate Schiff base ligands, the average of the four equatorial Mn–O and Mn–N distances hardly changes: 1.918, 1.923, 1.924, 1.923 Å, respectively. Even the drastic changes in the axial ligands appear to self-compensate with one O atom drawing nearer as the other becomes more distant; the average axial Mn–O distances in the four complexes are 2.303, 2.282, 2.246 and 2.298 Å. In the present structure, the single water molecule donates hydrogen bonds to perchlorate O(4) and (more strongly) to phenolate O(5) with H···O distances 2.18(3) and 1.95(3) Å, O···O distances 2.874(4) and 2.744(4) Å, O–H···O angles 148(5) and 165(5)°, respectively. Even though the comparison structure with water and methanol as ligands has one more polar H atom available for hydrogen bonding, the phenolato O atoms are not used as acceptors [28]. However, in the second comparison structure there are hydrogen bonds from water ligands to phenolato O atoms.

### 3.2.2. Complex 5 [MnL(OAc)]

An ORTEP diagram along with atom numbering scheme for the asymmetric unit of **5** is shown in Fig. 2. In the asymmetric unit the ligand L occupies the equatorial plane with the Mn–O and Mn–N distances very similar to that of **3**. The basal bond angles of the two molecules are also quite similar. The atoms Mn(1), O(2), N(1) and N(2) form a good least square plane with the Mn(1) atom showing the maximum deviation of 0.036(4) Å from this plane. The other donor atom in the basal plane O(1) is appreciably deviated from this plane (0.221(1) Å). The acetate ion is coordinated by one of its oxygen O(3) to the axial position and the Mn(1)–O(3) bond length is, as expected, appreciably longer than the equatorial Mn(1)–O(1) bond. However, the more interesting aspect of this structure is that the other oxygen of the acetate O(4) is also participating in coordination by binding to a second MnL moiety. Thus in the solid state, the Mn(1) atom is in a 4 + 2 coordination geometry and the acetate ion joins the individual distorted octahedrons to form a one dimensional infinite chain (see Fig. 3).

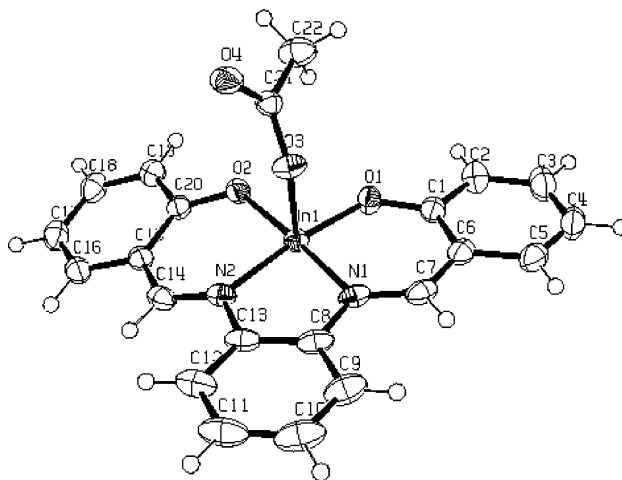


Fig. 2. ORTEP diagram and atom numbering scheme for the complex **5** [Mn(L)(OAc)] showing 50% probability ellipsoid for the non-hydrogen atom.

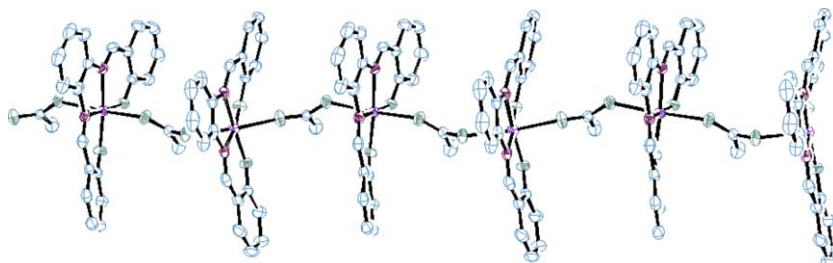


Fig. 3. A view of the linear chain of complex **5**.

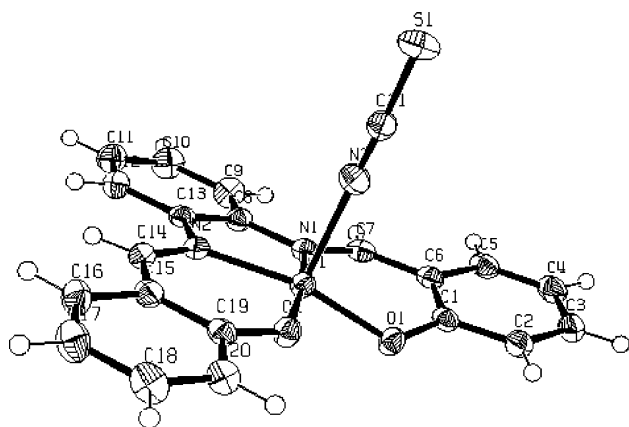


Fig. 4. ORTEP diagram and atom numbering scheme for the complex **13** [Mn(L)(NCS)] with 50% thermal probability ellipsoid for the non-hydrogen atom.

### 3.2.3. Complex **13** [MnL(NCS)]

The ORTEP representation of **13** (Fig. 4) shows that the Mn center is in a square pyramidal geometry. The Mn–O (phenolate) distances (average 1.8724 Å) and Mn–N (imine) distances (average 1.9894 Å) in **13** are similar to those observed in **3** and **5**. The manganese atom is additionally bound to a N-bonded thiocyanate anion in the axial position where the Mn–N bond distance is longer (2.1643 Å) than the usual due to Jahn–Teller distortion. The N–C–S angle is 178.08° indicates that the NCS is linear. It is interesting to note that though thiocyanate is a well-known bridging ligand, and we have solved the X-ray crystallographic structure of the molecule, with a hope to obtain a chain like structure, similar to that of the corresponding acetate complex **5**, the actual structure shows that no such chain exists in the solid state. The ‘hard’ coordination atmosphere of manganese(III) probably precludes the coordination of ‘soft’ sulfur of thiocyanate moiety and thus the chain formation cannot proceed.

### 3.3. Infrared spectra and magnetic moment

The IR spectra of all the complexes have several prominent bands. A strong band at ca. 1605  $\text{cm}^{-1}$  is assigned to  $\nu(\text{C}=\text{N})$  stretching vibration. Additional strong bands at ca. 1585, 1532 and 1450  $\text{cm}^{-1}$  have been previously assigned to  $\nu(\text{C}=\text{C}$ , phenyl ring),  $\nu(\text{C}=\text{N} + \text{C}=\text{C} + \text{C}=\text{O})$  stretching vibrations, respectively [31]. The perchlorate complexes **3** and **4** show a number of strong and broad bands with peaks at ca. 1106 and 1128  $\text{cm}^{-1}$  for **3** and at 1136 and 1055  $\text{cm}^{-1}$  for **4** together with bands at ca. 617, 638  $\text{cm}^{-1}$  for **3** and at 625, 636  $\text{cm}^{-1}$  for **4**, that are indicative of the presence of coordinated perchlorate. The  $\nu_{\text{a}}(\text{COO}^-)$  and  $\nu_{\text{s}}(\text{COO}^-)$  bands of acetate complexes **5** and **6** appear at ca. 1575 and 1430  $\text{cm}^{-1}$ , respectively. The strong vibrations at ca. 2100  $\text{cm}^{-1}$  of the thiocyanate complex

**13** may be attributable to the N-bonded thiocyanate [32]. For **14** and **15**, a strong peak at ca. 2040  $\text{cm}^{-1}$  have been shown to be diagnostic of anti symmetric stretch  $\nu_{\text{asym}}(\text{N}_3)$  vibrations. A broad absorption of most of the complexes at ca. 3430  $\text{cm}^{-1}$  is due to  $\nu(\text{H}_2\text{O})$  vibrations.

The analytical data of the complexes along with their room temperature magnetic moment data are given in Table 1. The value of magnetic moments for the complexes **1** and **2** are 5.92 and 6.01 BM, which are consistent with high-spin square pyramidal stereochemistry. Similarly, the magnetic susceptibility data for all manganese(III) complexes except **5** and **6** are in the range of 4.98–4.62 BM indicating high-spin  $d^4$  configuration. The much lower magnetic moment of **5** and **6** indicates that there is appreciable superexchange between the manganese(III) centers through the bridging acetate ions.

### 3.4. Electronic spectra

The electronic spectra (mull) of manganese(II) complexes exhibit (Table 5) lack of any characteristic absorption peak in the visible region, presumably because the weak d–d bands are submerged in the tail of the charge transfer bands. The spectra of all the manganese(III) complexes are very similar to those previously reported for closely related Mn(salen)(X) [21], Mn(acen)(X) [33] and other manganese(III) complexes [34]. The earlier workers have assigned the visible region of the spectra to d–d transitions of Jahn–Teller distorted  $d^4$  system, which under ideal symmetric ligand field will be  ${}^5\text{E} \rightarrow {}^5\text{T}$  transition. However, the complexes of the type being discussed here are of much lower symmetry ( $\text{C}_1$ ). Boucher and Coe [25] as well as Chaudhury and co-workers [34c] assumed a pseudo- $\text{C}_{4v}$  symmetry for

Table 5  
Electronic spectral data for the complexes

Complex	UV–Vis [ $\lambda_{\text{max}}$ (nm)]/ $\epsilon$ ( $\text{M}^{-1} \text{cm}^{-1}$ )
<b>1</b>	470, 400 (Nujol mull)
<b>2</b>	470, 410 (Nujol mull)
<b>3</b>	600(592), 550(1015), 445(8230), 340(23 870) 600, 560, 500 (Nujol mull)
<b>4</b>	600(647), 550(886), 438(5179) 338(14 242)
<b>5</b>	595(515), 540(925), 440(4925), 345(14 328) 600, 550, 500 (Nujol mull)
<b>6</b>	600(278), 550(618), 410(10 069), 320(11 850)
<b>7</b>	595(423), 545(1083), 440(6456), 340(17 977)
<b>8</b>	600(448), 550(1048), 425(8267), 340(17 507)
<b>9<sup>a</sup></b>	595(344), 545(964), 440(6010), 341(16 932)
<b>10<sup>a</sup></b>	600(405), 550(628), 440(2921), 340(8082)
<b>11</b>	600(408), 545(756), 445(8692), 345(18 002)
<b>12</b>	600(514), 550(838), 440(4852), 340(12 822)
<b>13</b>	595(420), 545(755), 425(11 000), 340(17 480)
<b>14</b>	590(429), 545(715), 430(6645), 340(18 750)
<b>15</b>	600(134), 550(1130), 405(8686), 325(17 064)

<sup>a</sup> In DMF and rests are in MeOH.

such systems, and they predicted three spin-allowed d–d transitions  ${}^5B_1 \rightarrow {}^5A_1$ ,  ${}^5B_1 \rightarrow {}^5E$  and  ${}^5B_1 \rightarrow {}^5B_2$  are possible, of which the first one will involve an electron from the  $d_z^2$  orbital and the spectra should be sensitive to the nature of the axial ligands. However, as the data tabulated in Table 5 show, the spectra of all the complexes are nearly the same and insensitive to the identity of the axial ligands. This may be due to the displacement of the axial ligands by coordinating solvent, viz., MeOH, but since the mull spectra of the complexes are nearly the same as solution spectra, and the complexes are non-conducting in nature in solution so the possibility of  ${}^5B_1 \rightarrow {}^5A_1$  transition is ruled out. So, the first band is due to the  ${}^5B_1 \rightarrow {}^5E$  transition and thus it is independent of energy of the  $d_z^2$  orbital. The second band is then due to the  ${}^5B_1 \rightarrow {}^5B_2$  transition. Beside the d–d transitions, the complexes exhibit two charge transfer bands in the near UV-region. The band at ca. 440 nm may be attributable to phenolate  $O(p_\pi) \rightarrow Mn(d_{\pi^*})$  ligand-to-metal charge transfer by analogy with related manganese(III) complexes. The remaining band at ca. 350 nm is most likely due to  $\pi \rightarrow \pi^*$  (azomethine) ligand transition. Though the electronic spectral assignments in the previous paragraph were done following the works on similar systems reported in the literature, in order to have a deeper understanding of the problem we have carried out UHF ZINDO/S calculations [35,27] on **5** and **13**.

Our calculations show that the HOMO to HOMO-3 orbitals containing the four unpaired electrons for these two molecules, contain at the most 2–3% Mn character as measured by the sum of square of the coefficients of the manganese orbitals in a given M.O. This is also nicely illustrated in Fig. 5, which clearly shows that the HOMO and SHOMO for **13** is mainly based on N atom of thiocyanate. We have recently observed similar results using more accurate ab initio GAMESS calculation [27]. Thus, the visible spectral bands are best assigned to HOMO  $\rightarrow$  LUMO and SHOMO  $\rightarrow$  LUMO transitions.

### 3.5. Electrochemical studies

The electrochemical properties of all the complexes have been investigated by cyclic voltammetry at a glassy carbon electrode. The experiments were carried out at room temperature in MeCN and DMF solution using 0.1 mol dm<sup>-3</sup>  $NEt_4 ClO_4$  as supporting electrolyte. The ligands  $LH_2$  and  $L/H_2$  are electro-inactive up to  $-1.5$  V. The cyclic voltammogram of Mn(II) complexes, **1** and **2**, have grossly identical features (Table 6), both the complexes showing one oxidative response nearly at 0.0 V assignable to Mn(II) to Mn(III) oxidation. The Mn(III)/Mn(II) couple for complex **2** is situated at more positive value compared to that of **1**, indicating that due to the presence of electronegative Br substituents in the ligand in **2**, the oxidation of Mn(II) becomes

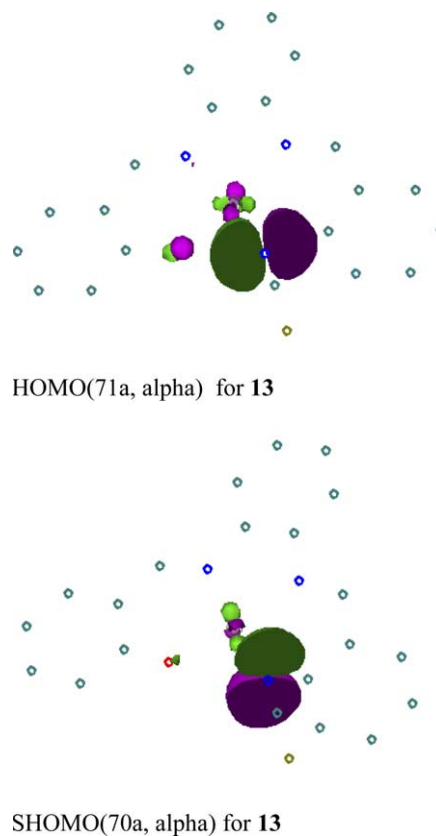


Fig. 5. HOMO(71a, alpha) for **13**. SHOMO(70a, alpha) for **13**.

Table 6  
Electrochemical data for the complexes

Complex	$E_{1/2}(Mn^{III}/Mn^{II})$ , $[\Delta E]$ (V) <sup>a</sup>	$E_{1/2}(Mn^{IV}/Mn^{III})$ , $[\Delta E]$ (V)
<b>1</b>	-0.08[0.122]	
<b>2</b>	-0.054[0.076]	
<b>3</b>	-0.021[0.074]	0.426[0.108]
<b>4</b>	0.160[0.172]	0.490[0.088]
<b>5</b>	0.06 <sup>b</sup>	0.444[0.070]
<b>6</b>	0.068[0.140]	0.491[0.060]
<b>7</b>	-0.092[0.086]	0.886[0.120]
<b>8</b>	0.050[0.124]	0.940[0.150]
<b>9<sup>a</sup></b>	-0.089(0.074)	0.487[0.094]
<b>10<sup>a</sup></b>	-0.071[0.066]	0.518[0.060]
<b>11</b>		
<b>12</b>	-0.045[0.105]	0.430 <sup>b</sup>
<b>13</b>		
<b>14</b>	-0.011[0.094]	0.485[0.122]
<b>15</b>	0.045[0.070]	0.510[0.144]

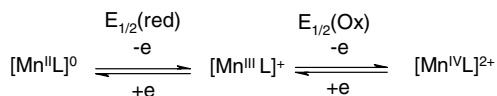
<sup>a</sup> DMF solvent and rest are in MeCN.

<sup>b</sup> Irreversible peak potentials, rest are quasi and reversible peak potentials, respectively.

\*  $E_{1/2} = (E_{pa} + E_{pc})/2$  V,  $\Delta E_p = |E_{pa} - E_{pc}|$  V, where  $E_{pa}$  and  $E_{pc}$  are anodic and cathodic peak potentials, respectively.

more difficult than in **1**, thus demonstrating an electronic effect on redox potential. The electron transfer properties of all Mn(III) complexes have grossly similar characteristics (Table 6). Most of the complexes display

one reductive and another oxidative response, tentatively assigned to Mn(III) → Mn(II) reduction and Mn(III) → Mn(IV) oxidation, respectively. This type of observation where manganese(III) shows both oxidation and reduction has also been found earlier [34c] although there are some exception where manganese(III) show only Mn(III) → Mn(II) reduction [36]. In all the cases when the redox potential of the complexes of L' containing the bromo-substituent salicylidene moiety is compared with the analogous complexes of L, the former complex always have higher  $E_{1/2}$  value than the later, indicating the stabilization of the lower oxidation state by the L' ligand. Comparison of the  $E_{1/2}$  values for the Mn(IV)/Mn(III) couple, between **7** and **9** and between **8** and **10**, indicate that more polarizable bromide ligand makes the Mn(III) → Mn(IV) oxidation easier (less positive  $E_{1/2}$  value) [37] compared to much less polarizable chloride, because bromide transfer more electron density to the metal center than chloride. However, the  $E_{1/2}$  values for the Mn(III)/Mn(II) couple for these complexes are too close to each other to make any such comparison, considering the fact that for **7** and **8** the data was obtained in MeCN where as for **9** and **10** it was in DMF. As the oxidation involves removal of an electron from  $d_z^2$  orbital, while during reduction the electron is added to  $d_{xy}$  orbital, so effect of axial ligand is expected to be more pronounced on oxidation than on reduction. Due to lack of solubility of bromo complexes (**9** and **10**) in MeCN, we have run the voltammetric experiments in DMF and we have the voltammograms, which have identical features like other complexes.



Cyclic voltammograms of azide complexes **14** and **15** exhibit a quasi-reversible Mn(III) → Mn(IV) metal centered oxidation process in the positive potential region (Fig. 6) and a quasi-reversible/reversible Mn(III) →

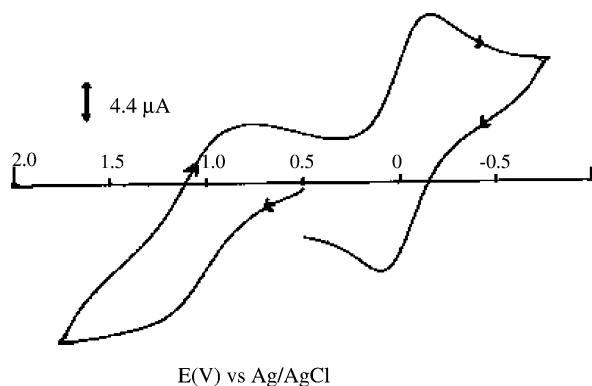


Fig. 6. Cyclic of **8** [Mn(L')(Cl)(H<sub>2</sub>O)] in MeCN with 0.1 mol dm<sup>-1</sup> NEt<sub>4</sub>ClO<sub>4</sub> as supporting electrolyte (working electrode, Glassy-Carbon; reference electrode, Ag/AgCl; Scan rate 100 mV s<sup>-1</sup>).

Mn(II) reduction process. The redox behavior of iodo complex involving the L' ligand **12** shows an irreversible oxidation at +0.43 V and a quasi-reversible reduction at -0.04 V. A comparison of the electrochemical data (Table 6), reveals that the complexes with electron withdrawing substituent directly attach to the manganese(III) center get more difficult to oxidize than the complexes where the electron withdrawing group attached to the ligand moiety.

Though the redox properties discussed above have been described as metal-based redox reactions following similar assignments of previous workers, the results of ZINDO/S calculations suggest that they should better be discussed in terms of electron addition to HOMO-3 for reduction and electron removal from HOMO for the oxidation process.

#### 4. Computational method

Single point ZINDO/S calculations were carried out on the manganese complexes using UHF method, with the help of HYPERCHEM 7.01 program[38], with the default parameters of the program ( $\sigma$ - $\sigma$  overlapping factor 1.267,  $\pi$ - $\pi$  overlapping factor 0.585, convergence limit 0.01). The geometries of the complexes **3** and **5** for the single point ZINDO/S calculations were taken directly from the crystal structure.

#### Acknowledgments

Financial assistance from UGC, CSIR and AICTE is gratefully acknowledged. S.B. thanks CSIR for award for a SRF. The authors thank the AICTE-MODROBS program for the purchase of the electrochemical unit. Authors acknowledge the help of D.O. Miller, Department of Chemistry, Memorial University of Newfoundland, for X-ray crystallography and Dr. Bob McDonald, Department of Chemistry, University of Alberta for data collection. We also thank DST-FIST program for providing FTIR and UV-Vis Spectrophotometer.

#### Appendix A. Supplementary data

Crystallographic data for the structure analysis have been deposited with the Cambridge Crystallographic Data, CCDC Nos. are 240638 (**3**), 238882 (**5**) and 238883 (**13**). Copy of the data can be obtained, free of charge, on application to the CCDC, 12 Union Road, Cambridge CB2 1 EZ, UK (fax: +44 1223 336033 or e-mail: deposit@ccdc.cam.ac.uk). Supplementary data associated with this article can be found, in the online version, at doi:10.1016/j.ica.2005.01.026.

## References

- [1] V.L. Pecoraro (Ed.), *Manganese Redox Enzymes*, VCH, New York, 1992.
- [2] G. Christou, *Acc. Chem. Res.* 22 (1989) 328.
- [3] K. Wieghardt, *Angew. Chem., Int. Ed. Engl.* 28 (1989) 1153.
- [4] L. Que, A.E. True, *Prog. Inorg. Chem.* 38 (1990) 97.
- [5] K. Sauer, *Acc. Chem. Res.* 13 (1980) 249.
- [6] Govindjee, W. Coleman, *Sci. Am.* 260 (1990) 50.
- [7] G. Renger, *Angew. Chem., Int. Ed. Engl.* 26 (1987) 643.
- [8] W.F. Bayer Jr., I. Fridovich, *Biochemistry* 24 (1985) 6460.
- [9] Y. Kono, I. Fridovich, *J. Biol. Chem.* 258 (1983) 6015.
- [10] I. Fridovich, *Acc. Chem. Res.* 15 (1982) 200.
- [11] (a) J.S. Vallentine, D. Motade Freitas, *J. Chem. Educ.* 62 (1985) 990;  
(b) M.G.B. Drew, C.J. Harding, V. McKee, G.G. Morgan, J. Nelson, *J. Chem. Soc., Chem. Commun.* (1995) 1035.
- [12] K. Srinivasan, P. Michaud, J.K. Kochi, *J. Am. Chem. Soc.* 108 (1986) 2309.
- [13] M. Ray, S. Mukherjee, R.N. Mukherjee, *J. Chem. Soc., Dalton Trans.* (1990) 3635.
- [14] Y.R. Sharma, P.K.S. Prakash, *Ind. J. Chem.* 19A (1980) 1175.
- [15] P.A. Goodson, A.R. Oki, J. Glerup, D.J. Hodgson, *J. Am. Chem. Soc.* 112 (1990) 6248.
- [16] (a) P.M. Plaksin, R.C. Stoufer, M. Mathew, G.J. Palenik, *J. Am. Chem. Soc.* 94 (1972) 2121;  
(b) M. Devereux, M. McCanm, V. Leon, M. Geraghty, V. McKee, J. Wikaira, *Polyhedron* 19 (2000) 1205;  
(c) W. Sun, H. Wang, C. Xia, J. Li, P. Zhao, *Angew. Chem., Int. Ed. Engl.* 42 (2003) 1042.
- [17] Y. Gultneh, T.B. Yisgedu, Y.T. Tesema, R.J. Butcher, *Inorg. Chem.* 42 (2003) 1857.
- [18] A. Gref, G. Balavoine, H. Riviere, C.P. Andrieux, *Nuov. J. Chim.* 8 (1984) 615.
- [19] R. Ramrai, A. Kira, M. Kaneko, *Angew. Chem., Int. Ed. Engl.* 25 (1986) 825.
- [20] D.T. Sawyer, A. Sobkowiak, J.L. Roberts Jr., *Electrochemistry for Chemists*, second ed., John Wiley & Sons, New York, 1995, p. 333.
- [21] H. Torayama, T. Nishide, H. Asada, M. Fujiwara, T. Matsushita, *Polyhedron* 17 (1998) 105.
- [22] Data were processed using the program XCAD4B (K. Harms, University of Marburg) and the commercial package SHELXTL-PLUS Release 5.05/V © 1996 Siemens Analytical X-Ray Instruments, Inc., Madison, WI.
- [23] G.M. Sheldrick, SHELXS-86, Program for the Solution of Crystal Structures, University of Göttingen, Germany, 1986.
- [24] G.M. Sheldrick, SHELX-97, 1997.
- [25] L.J. Boucher, C.G. Coe, *Inorg. Chem.* 15 (1976) 1334.
- [26] (a) A. Böttcher, H. Elias, E.G. Jäger, H. Langfelderova, M. Mazur, L. Müller, H. Paulus, P. Pelikan, M. Rudolph, M. Valko, *Inorg. Chem.* 32 (1993) 4131;  
(b) O. Horner, E.A. -Mallart, M.-F. Charlot, L. Tchertanov, J. Guilhem, T.A. Mattioli, A. Boussac, J.-J. Girerd, *Inorg. Chem.* 38 (1999) 1222.
- [27] S. Naskar, S. Biswas, D. Mishra, B. Adhikary, L.R. Falvello, T. Soler, C.H. Schwalbe, S.K. Chattopadhyay, *Inorg. Chim. Acta* 357 (2004) 4257.
- [28] T. Fukuda, F. Sakamoto, M. Sato, Y. Nakano, X.S. Tan, Y. Fuji, *J. Chem. Soc., Chem. Commun.* (1998) 1391.
- [29] N. Aurangzeb, C.E. Hulme, C.A. McAuliffe, R.G. Pritchard, M. Watkinson, M.R. Bermejo, A. Garcia-Deibe, M. Rey, J. Sanmartin, A. Sousa, *J. Chem. Soc., Chem. Commun.* (1994) 1153.
- [30] Y. Ciringh, S.W. Gordon-Wylie, R.E. Norman, G.R. Clark, S.T. Weintraub, C.P. Horwitz, *Inorg. Chem.* 36 (1997) 4968.
- [31] S.K. Mondal, P. Paul, R. Ray, K. Nag, *Trans. Met. Chem.* 9 (1984) 247.
- [32] R.A. Bailey, S.L. Kozak, T.W. Michelsen, W.N. Mills, *Coord. Chem. Rev.* 6 (1971) 407.
- [33] L.J. Boucher, V.W. Day, *Inorg. Chem.* 16 (1977) 1360.
- [34] (a) R. Dingle, *Acta Chem. Scand.* 20 (1966) 33;  
(b) R.K. Boggess, J.W. Hughes, W.M. Coleman, L.T. Taylor, *Inorg. Chim. Acta* 38 (1980) 183;  
(c) S.B. Kumar, S. Bhattacharyya, S.K. Dutta, E.T. Tiekink, M. Chaudhury, *J. Chem. Soc., Dalton Trans.* (1995) 2619.
- [35] (a) J.E. Ridley, M.C. Zerner, *Theor. Chim. Acta* 42 (1976) 223;  
(b) A.D. Bacon, M.C. Zerner, *Theor. Chim. Acta* 53 (1979) 21.
- [36] (a) M.R. Bermejo, A. Castiñeiras, J.C.G. -Monteagudo, M. Rey, A. Sousa, M. Watkinson, C.A. McAuliffe, R.G. Pritchard, R.L. Beddoes, *J. Chem. Soc., Dalton Trans.* (1996) 2935;  
(b) M. Maneiro, M.R. Bermejo, A. Sousa, M. Fondo, A.M. González, A.S. -Pedrares, C.A. McAuliffe, *Polyhedron* 19 (2000) 47;  
(c) A. Panja, N. Shaikh, M. Ali, P. Vojtišek, P. Banerjee, *Polyhedron* 22 (2003) 1191.
- [37] W.M. Coleman, R.R. Goehring, L.T. Taylor, J.G. Mason, R.K. Boggess, *J. Am. Chem. Soc.* 101 (1979) 2311.
- [38] Hyperchem for Windows, Release 7.01, Hypercube Inc., Gainesville, FL.